Acoustic localization in weakly compressible elastic media containing random air bubbles

Bin Liang and Jian-chun Cheng*
Laboratory of Modern Acoustics and Institute of Acoustics, Nanjing University, Nanjing 210093, People's Republic of China
(Received 8 June 2006; published 10 January 2007)

We study theoretically the propagation of longitudinal wave in weakly compressible elastic media containing random air bubbles by using a self-consistent method. By inspecting the scattering cross section of an individual bubble and estimating the mean free paths of the elastic wave propagating in the bubbly weakly compressible media, the mode conversion is numerically proved negligible as the longitudinal wave is scattered by the bubbles. On the basis of the bubble dynamic equation, the wave propagation is solved rigorously with the multiple scattering effects incorporated. In a range of frequency slightly above the bubble resonance frequency, the acoustic localization in such a class of media is theoretically identified with even a very small volume fraction of bubbles. We present a method by analyzing the spatial correlation of wave field to identify the phenomenon of localization, which turns out to be effective. The sensibility of the features of localization to the structure parameters is numerically investigated. The spatial distribution of acoustic energy is also studied and the results show that the waves are trapped within a spatial domain adjacent to the source when localization occurs.

DOI: 10.1103/PhysRevE.75.016605 PACS number(s): 43.20.+g, 02.60.−x, 45.05.+x

I. INTRODUCTION

Considerable efforts have been and continue to be devoted to the research of the propagation of classical waves in random media. Under appropriate conditions, a ubiquitous phenomenon of wave localization may arise from the multiple scattering of waves in random media. The concept of localization was first proposed by Anderson about half a century ago for the electronic mobility [1]. Later the phenomenon of localization has also been reported for microwaves [2,3] and for light [4,5] in inhomogeneities. Sornette and Souillard suggested the localization of acoustic waves in bubbly liquids but gave no detailed result [6]. The sound wave propagation in bubbly water was investigated theoretically by Ye *et al.* using a self-consistent method [7–12]. Their numerical results confirmed that for a range of frequencies the wave localization can be achieved in bubbly liquid with even a very small fraction of bubbles. However, bubbles in liquids are highly flowable and instable, it is thus inconvenient to confirm experimentally the existence of acoustic localization in bubbly liquids. In this context, the question seems to be reasonable: Is acoustic localization a ubiquitous phenomenon in a bubbly solid with better stability? But the answer is generally negative; air bubbles in usual solids cannot act effectively as strong acoustic scatterers, lacking the resonant characteristic as in liquids. Due to high value of shear modulus, the bubble oscillation will be attenuated in a time comparable with its period, which can be easily seen from the formula for the oscillation frequency of a bubble in isotropic media [13].

There exists a class of "weakly compressible" media that may be called waterlike for which the inequalities $\lambda \gg \mu$ are fulfilled [14,15] e.g., a tissuelike gel or soft rubber. Here λ and μ are the Lamé coefficients. Such weakly compressible media with small shear stiffness is dynamically similar to liquids to a great extent [16]. The dynamics of an individual bubble in weakly compressible media has been investigated by Ostrovsky [14,15], Zabolotskaya *et al.* [16], and Liang *et al.* [17]. The bubble oscillation in this class of media is somewhat special, due to the fact that only if the ratio λ/μ is sufficiently large can a bubble behave like an oscillator with a large quality factor [15]. Indeed, the bubble dynamic equations for weakly compressible media [14–17] are quite similar in form to the one for liquids, i.e., the well-known Rayleigh-Plesset equation. Consequently, we expect the potential occurrence of acoustic localization in weakly compressible media containing air bubbles under appropriate conditions that may serve as a more effective model for an experimental verification than bubbly liquids. In the present paper, the propagation of longitudinal acoustic wave in such a class of media is investigated, in which the mode conversion is numerically proved negligible. Based on the radial pulsation equation of a single bubble, the wave propagation is formulated in terms of a set of self-consistent equations and then solved rigorously. Theoretical results show that acoustic localization can be achieved in a range of frequency. We present a method to identifying the localization effectively by properly analyzing the spatial correlation behaviors of wave field.

II. THEORY

A. The model

Consider a longitudinal wave in a weakly compressible medium containing air bubbles with small volume fraction β. In the present study, the weakly compressible medium is regarded as elastic, with the purpose of excluding the effects of absorption that may lead to ambiguity in data interpretation [9]. We shall restrict our attention to the wave propagation at low frequencies, i.e., $kr_0 \ll 1$. Here $k=\omega/c_l$ and $c_l = \sqrt{(\lambda+2\mu)/\rho}$ are the wave number and the speed of the

*Author to whom correspondence should be addressed. Electronic mail: jccheng@nju.edu.cn

longitudinal wave, respectively, and ρ is the mass density. We assume that the wave is emitted from a unit point source and of angular frequency ω. The emission source is assumed to be at the origin, surrounded by N spherical air bubbles that are randomly located at $\boldsymbol{r}_i$ in a not overlapping way with $i=1,2,\ldots,N$. For simplicity and without loss of generality, all the bubbles are assumed to be of uniform radius r_0 and randomly distributed within a spatial domain, which is taken as the spherical shape so as to eliminate irrelevant effects due to an irregular edge. Then the radius of the spherical bubble cloud is $R=(N/\beta)^{1/3}r_0$. Here the source is placed inside rather than outside the bubble cloud, which is the only way to isolate the localization effect from boundary effects and unambiguously investigate the problem of whether the transmitted waves can indeed be trapped [10].

B. Validation of the approximation

As the incident longitudinal wave is scattered by a bubble in weakly compressible media, the energy converted into shear wave can be expected negligible, on condition of sufficiently small shear stiffness. Indeed, the scattered shear wave produced by a single bubble in weakly compressible media was not taken into account by Ostrovsky [14,15] and Zabolotskaya [16]. Next we shall present a numerical demonstration of the validation of such an approximation by inspecting the scattering cross section of a single bubble in weakly compressible media.

The total scattering cross section σ of a single bubble can be expressed as $\sigma=\sigma_L+\sigma_S$, where σ_L and σ_S refer to the contributions of the scattered longitudinal and shear waves, respectively. Therefore it is conceivable that the ratio σ_L/σ_S actually reflects the extent to which the mode conversion will occur as the incident longitudinal wave is scattered by the bubble. The value of σ_L/σ_S can be readily obtained from Eq. (19) in Ref. [18].

A series of numerical experiments has been performed for an individual bubble in a variety of media, for the purpose of investigating how the energy converted into shear wave is affected as the media of matrix varies. Figure 1 presents the typical result of the comparison between the ratios σ_L/σ_S versus frequency kr_0 for different media of matrix. Three particular kinds of weakly compressible elastic media are considered: Agar-gelatin, plastisol, and gelatin. Aluminum is also considered for comparison. The physical parameters of these materials are listed in Table I. Note that the physical parameters of weakly compressible elastic media approximate to those of water except for different values of shear moduli, which seems to be natural for such "waterlike" media.

From Fig. 1, we find: (1) the energy of the scattered shear wave is extremely small when compared to that of the scattered longitudinal wave, as long as the ratios λ/μ are sufficiently large. Contrarily the magnitude of the longitudinal components is nearly the same to the shear components in the scattered field for μ comparable with λ. (2) For an individual bubble in different weakly compressible media, the energy converted into shear wave is diminished as the shear modulus of the medium of matrix decreases, as expected. (3)

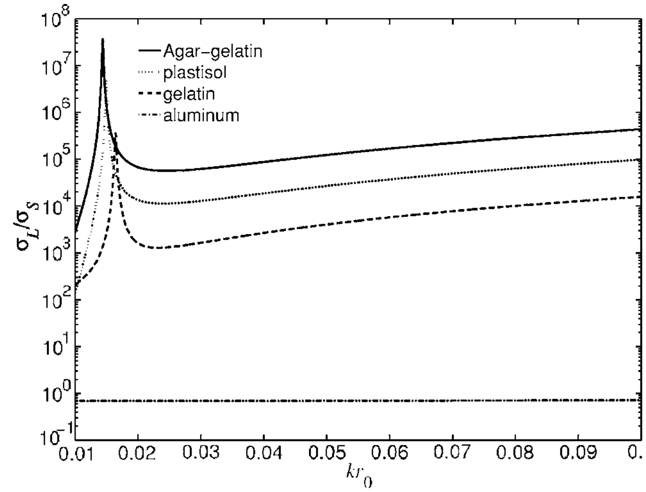

FIG. 1. The ratio σ_L/σ_S versus frequency kr_0 for a single bubble in different materials.

Moreover, the ratios σ_L/σ_S are greatly enhanced in the proximity of the natural resonance of the individual bubbles, owing to the giant monopole resonance that is the dominant mode of bubble pulsation at low frequencies [19].

Thereby it follows that the energy converted into shear waves is insignificant as the incident longitudinal wave is scattered by a bubble in weakly compressible media. The shear component of the scattered field may thus be expected to be negligible as the longitudinal wave propagates in a bubbly weakly compressible medium. It should be stressed, however, that such an approximation can only be regard valid under the condition that the propagation of the elastic waves is not completely diffusive. Otherwise there will be an entirely contradicting conclusion that the ratio between the energy of the shear and the longitudinal wave is as large as $2(c_l/c_s)^3$ when the wave field is completely diffusive [20,21]. Here $c_s=\sqrt{2\mu/\rho}$ is the speed of the shear wave.

Such a seeming paradox may be clarified by estimating the ratio between the mean free path (MFP) of the wave and the linear "sample size" R of the random medium. For a classical wave propagating in a random media, the transport MFP is defined as the length over which momentum transfer becomes uncorrelated, while the elastic MFP is the average distance between two successive scattering events [22]. For the longitudinal wave, the transport MFP l_{T_l} and the elastic MFP l_{E_l} are defined as below [23]

TABLE I. The physical parameters of the materials

Materials	ρ (kg/m^3)	λ	μ	λ/μ
Agar-gelatin[a]	1000	2.25 GPa	6.35 KPa	4×10^5
plastisol[b]	1000	2.55 GPa	12.1 KPa	2×10^5
gelatin[c]	1000	2.25 GPa	39.0 KPa	5×10^4
aluminum	2700	111.3 GPa	37.1 GPa	3

[a]Reference [29].
[b]References [15,30,31].
[c]Reference [16].

$$l_{T_l}=\frac{2r_0^3}{3\beta}\left(\int_0^{\pi}|f_{pp}(\theta)|^2\sin\theta(1-\cos\theta)d\theta\right)^{-1},$$

$$l_{E_l}=\frac{2r_0^3}{3\beta}\left(\int_0^{\pi}|f_{pp}(\theta)|^2\sin\theta d\theta\right)^{-1},$$

where the parameter of $f_{pp}(\theta)$ is the scattering amplitude of the longitudinal wave that can be obtained from Eq. (19) in Ref. [24]. Similarly, the transport MFP l_{T_s} and the elastic MFP l_{E_s} of the shear wave can be defined as follows:

$$l_{T_s}=\frac{2r_0^3}{3\beta}\left(\int_0^{2\pi}\int_0^{\pi}|f_{ss}(\theta,\varphi)+f_{tt}(\theta,\varphi)|^2\times\sin\theta(1-\cos\theta)d\theta d\varphi\right)^{-1},$$

$$l_{E_s}=\frac{2r_0^3}{3\beta}\left(\int_0^{2\pi}\int_0^{\pi}|f_{ss}(\theta,\varphi)+f_{tt}(\theta,\varphi)|^2\sin\theta d\theta d\varphi\right)^{-1},$$

where the parameters of $f_{ss}(\theta,\varphi)$ and $f_{tt}(\theta,\varphi)$ are the scattering amplitudes of the shear wave that can be obtained from Eq. (20) in Ref. [25]. It is observable from Refs. [18,24,25] that the scattering cross sections and the scattering amplitudes of the elastic wave are described in terms of the series expansions. Therefore numerical errors are inevitable as these series expansions are truncated in the numerical experiments. It has been proved, however, that it is sufficient to describe the wave by just the first three terms of these series expansions at the low frequencies [26].

For an elastic wave, the following inequality has to be fulfilled to completely attain the diffusive regime [27]

$$1/k\ll l_{T_l}\ll R,\quad 1/\kappa\ll l_{T_s}\ll R,$$

where $\kappa=\omega/c_s$ is the wave number of the shear wave. Otherwise the wave propagation will be predominantly ballistic as the ratio between the MFP and the sample size is large [28].

At low frequencies from $kr_0=0$ to 0.1, a set of numerical experiments have been carried out to estimate the MFPs of the elastic waves in various bubbly weakly compressible media for all the structure parameters employed in the present study. The typical values of the sample size are roughly $R\sim 0.1$ m. The numerical calculations indicate that: (1) for the shear wave in bubbly weakly compressible media, the typical values of the transport MFP l_{T_s} and the elastic MFP l_{E_s} are approximately $l_{T_s},l_{E_s}\sim 10^2$ m. For any particular set of structure parameters, both the transport MFP l_{T_s} and the elastic MFP l_{E_s} are much larger than the sample size, i.e., $l_{E_s},l_{T_s}\gg R$. This manifests that the scattering of the low-frequency shear wave by the bubbles in a weakly compressible medium is weak and, therefore, the propagation of the shear wave in such a medium is ballistic rather than diffusive. (2) For the longitudinal wave, the relation $l_{E_l},l_{T_l}\gg R$ holds for any particular set of structure parameters, except for a frequency range within which $l_{T_l}\sim 0.1$ m and the Ioffe-Regel criterion $kl_{T_l}\le 1$ is satisfied [23]. As will be explained later, such a frequency range is in fact the region where the phenomenon of acoustic localization occurs. This is consistent with the conclusion regarding a bubbly liquid that the coherent wave dominates the transmission for most frequencies except for the localization region [7].

As a result, the condition to attain a completely diffusive wave field cannot be satisfied at low frequencies as the longitudinal wave propagates in a bubbly weakly compressible medium. Consequently, the shear component of the scattered field is unimportant when compared to the longitudinal component, and neglect of mode conversion only leads to negligible errors. The results of the numerical experiments indicate that the numerical error caused by neglecting mode conversion is less than 1% as long as the ratio λ/μ is roughly larger than 10^4. In the following study, we shall assume the scattered field to be totally longitudinal without taking mode conversion into consideration.

C. The bubble dynamics

For an individual bubble in weakly compressible elastic media, the radial pulsation driven by a plane longitudinal wave is described by a Rayleigh-Plesset-like equation, as follows [14,15]:

$$\frac{d^2U}{dt^2}+\omega_0^2U-\frac{r_0}{c_l}\frac{d^3U}{dt^3}=GU^2+q\left[2U\frac{d^2U}{dt^2}+\left(\frac{dU}{dt}\right)^2\right]-ep_{inc},\tag{1}$$

where $U=4\pi(r_{in}^3-r_0^3)/3$ is volume perturbation of an individual bubble with r_{in} being the instantaneous radius, p_{inc} refers to the incident plane wave on the bubble, i.e., the driving force of the bubble pulsation, $\omega_0=\sqrt{\omega_1^2+\omega_2^2}$ is the bubble resonance frequency with $\omega_1=\sqrt{4\mu/\rho r_0^2}$ and $\omega_2=\sqrt{3\rho_a c_a^2/\rho r_0^2}$ corresponding to the Meyer-Brendel-Tamm resonance and the Minnaert bubble resonance, respectively [32], the parameters of G, q, and e are given as $G=(9+2\chi)q\omega_0^2/2$, $q=1/(8\pi r_0^3)$, $e=4\pi r_0/\rho$. Here χ is a coefficient of asymmetry, which must lie in the range $0<\chi\le 1$. For a spherical bubble $\chi=1$. Up to the first order approximation, one obtains the harmonic solution of Eq. (1), as follows:

$$U=-\frac{4\pi r_0}{\rho(\omega_0^2-\omega^2-i\omega^3r_0/c_l)}p_{inc}.\tag{2}$$

At low frequencies, the acoustic field produced by acoustic radiation from a single bubble is taken to be the diverging spherical wave [16]

$$p_s(\boldsymbol{r},t)=p_s(\boldsymbol{r})\exp(-i\omega t)\approx-\frac{1}{4\pi r}\frac{d^2}{dt^2}U\left(t-\frac{r}{c_l}\right).\tag{3}$$

We assume that the bubble is the ith bubble located at $\boldsymbol{r}_i$ and express the incident plane wave as

$$p_{inc}(\boldsymbol{r},t)=p_{inc}(\boldsymbol{r})\exp(-i\omega t).\tag{4}$$

Substituting Eqs. (2) and (4) in Eq. (3) and discarding the time factor $\exp(-i\omega t)$, one obtains the scattered wave at $\boldsymbol{r}$ from the ith bubble, denoted by $p_s^i(\boldsymbol{r})$, as follows:

$$p_s^i(\boldsymbol{r}) = f p_{inc}(\boldsymbol{r}_i) G_0(\boldsymbol{r}-\boldsymbol{r}_i), \tag{5}$$

where $G_0(\boldsymbol{r}-\boldsymbol{r}_i)=\exp(ik|\boldsymbol{r}-\boldsymbol{r}_i|)/|\boldsymbol{r}-\boldsymbol{r}_i|$ is the usual three-dimensional Green's function, f is the scattering function of a single bubble, defined as

$$f = \frac{r_0}{(\omega_0^2/\omega^2 - 1 - ikr_0)}. \tag{6}$$

Equations (5) and (6) clearly show that the scattered fields and scattering function of a single bubble in weakly compressible media take an identical form as in liquid media, except for different expressions of ω_0 (see Eqs. (3) and (4) in Ref. [7] and also Eq. (2) in Ref. [11]). Compared with the resonance frequency of a bubble in liquid media that includes only the Minnaert contribution ω_2, an additional term ω_1 is present in Eq. (6), due to the contribution of shear wave in the solid wall of bubble. In the limiting case $\lambda/\mu \to \infty$, the weakly compressible medium becomes a liquid medium, and Eq. (6) degenerates to Eq. (4) in Ref. [7] due to the vanishing of ω_1. Despite such an agreement of the results in the form, we have to particularly stress that it is the radial pulsation equation of a single bubble from which the present theory begins, rather than the well-studied scattering function of a bubble employed in Ref. [7].

D. The self-consistent formalism

Among many useful formalisms suggested for describing the acoustic scattering by a finite group of random scatterers, the self-consistent method is proved to be particularly effective [33]. This method is based on a genuine self-consistent scheme proposed first by Foldy [34] and reviewed in Ref. [35]. Later Ye *et al.* employed the self-consistent method to investigate the wave propagation in a bubble liquid [7]. In the method, the multiple scattering of waves is represented by a set of coupled equations, and the rigorous results can be obtained by solving the equations. In the present study, the wave propagation in a bubbly weakly compressible medium will be solved by using the self-consistent method in an exact manner.

In the presence of bubbles, the radiated wave from the source is subject to multiple scattering by the surrounding bubbles. Hence the total acoustic wave at a spatial point $\boldsymbol{r}$ is supposed to include the contributions from the wave directed from the source and the scattered waves from all bubbles, i.e.,

$$p(\boldsymbol{r}) = p_0(\boldsymbol{r}) + \sum_{i=1}^{N} p_s^i(\boldsymbol{r}). \tag{7}$$

Analogously, the incident wave upon the ith bubble should consist of the direct wave from the source and the scattered waves from all bubbles except for itself, i.e., [35]

$$p_{inc}(\boldsymbol{r}_i) = p_0(\boldsymbol{r}_i) + \sum_{j=1, j\neq i}^{N} p_s^j(\boldsymbol{r}_i). \tag{8}$$

At $kr_0 \ll 1$, the dimension of bubbles is very small when compared to the wavelength, and the plane wave approximation still stands for the incident wave upon an individual bubble. In this situation, the dynamics of an individual bubble can be described by the radial pulsation equation given by Eq. (1). Therefore for the ith bubble, according to Eqs. (5) and (8), the following self-consistent equation should be satisfied

$$p_s^i(\boldsymbol{r}) = f\left[p_0(\boldsymbol{r}_i) + \sum_{j=1, j\neq i}^{N} p_s^j(\boldsymbol{r}_i) \right] G_0(\boldsymbol{r}-\boldsymbol{r}_i). \tag{9}$$

Upon incidence, each bubble acts effectively as a secondary pulsating source. The scattered wave from the ith bubble is regarded as the radiated wave and is rewritten as [11]

$$p_s^i(\boldsymbol{r}) = A_i G_0(\boldsymbol{r}-\boldsymbol{r}_i), \tag{10}$$

where the complex coefficient A_i refers to the effective strength of the secondary source. Substitution of Eq. (10) in Eq. (8) yields

$$A_i = f\left[p_0(\boldsymbol{r}_i) + \sum_{j=1, j\neq i}^{N} A_j G_0(\boldsymbol{r}_j-\boldsymbol{r}_i) \right]. \tag{11}$$

By setting $\boldsymbol{r}$ in Eq. (10) to any bubble other than the ith, this equation becomes a set of closed self-consistent equations which can be expressed as

$$\mathbf{A} = f\mathbf{P} + \mathbf{C}\mathbf{A}, \tag{12}$$

where $\mathbf{A}=[A_1, A_2, \ldots, A_N]^T$, $\mathbf{P}=[p_0(\boldsymbol{r}_1), p_0(\boldsymbol{r}_2), \ldots, p_0(\boldsymbol{r}_N)]^T$, $\mathbf{C}$ is an $N\times N$ matrix, defined as

$$\mathbf{C} = \begin{bmatrix} C_{11} & \cdots & C_{1N} \\ \vdots & \ddots & \vdots \\ C_{N1} & \cdots & C_{NN} \end{bmatrix},$$

where $C_{ij}=(1-\delta_{ij}) f G_0(\boldsymbol{r}_j-\boldsymbol{r}_i)$ with δ_{ij} being the Kronecker symbol. It is apparent that $\mathbf{C}$ is symmetric according to the principle of reciprocity. One may readily obtain from Eq. (12)

$$\mathbf{A} = f(1-\mathbf{C})^{-1}\mathbf{P}. \tag{13}$$

For an arbitrary configuration of the bubble distribution, the acoustic field in any spatial point may thus be solved exactly from Eqs. (7), (10), and (13). It is obvious that the multiple scattering effects have been incorporated during the computation [7].

E. The spatial correlation function

With the purpose of identifying efficiently the phenomenon of localization, we consider the spatial correlation that physically describes the interaction between the wave fields at different spatial points. For an arbitrary spatial point $\boldsymbol{r}$, the wave field is normalized as $T(r)=p(r)/p_0(r)$ to eliminate the uninteresting geometrical spreading factor. Here $r=|\boldsymbol{r}|$ is the distance from the source point to the spatial point, $p(r)$ refers to the acoustic pressure averaged over the sphere of radius r, and $p_0(r)=\exp(ikr)/r$ refers to the propagating wave radiated from the source in the absence of bubbles.

Consider the interaction between the two spatial points $\boldsymbol{r}+\boldsymbol{r}'/2$ and $\boldsymbol{r}-\boldsymbol{r}'/2$, as shown in Fig. 2. The spatial correla-

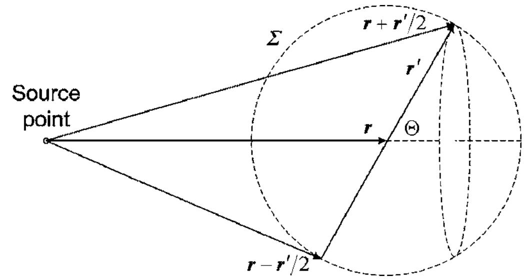

FIG. 2. Geometry for spatial correlation function of wave fields at $\boldsymbol{r}+\boldsymbol{r}'/2$ and $\boldsymbol{r}-\boldsymbol{r}'/2$.

tion is defined as the average over the sphere $\boldsymbol{\Sigma}$ that is located at $\boldsymbol{r}$ and of radius $\xi/2$. Here $\xi=|\boldsymbol{r}'|$ is the distance between $\boldsymbol{r}+\boldsymbol{r}'/2$ and $\boldsymbol{r}-\boldsymbol{r}'/2$. Note that the normalized wave field $T(r)$ is axially symmetric about $\boldsymbol{r}$ and depends only on Θ. The average can thus be accomplished by performing the integration with respect to Θ. Then the spatial correlation function is expressed as follows:

$$g(\boldsymbol{r}+\boldsymbol{r}'/2,\boldsymbol{r}-\boldsymbol{r}'/2) = \frac{\int_0^\pi 2\pi\langle T(|\boldsymbol{r}+\boldsymbol{r}'/2|)T^*(|\boldsymbol{r}-\boldsymbol{r}'/2|)\rangle\cdot(\xi/2)^2\sin\Theta\, d\,\Theta}{4\pi(\xi/2)^2} = \frac{1}{2}\int_0^\pi \langle T(|\boldsymbol{r}+\boldsymbol{r}'/2|)T^*(|\boldsymbol{r}-\boldsymbol{r}'/2|)\rangle \sin\Theta d\Theta, \tag{14}$$

where $|\boldsymbol{r}\pm\boldsymbol{r}'/2|=\sqrt{r^2+\xi^2/4\pm\xi r\cos\Theta}$, and $\langle\cdot\rangle$ refers to the ensemble average carried over random configuration of bubble clouds.

It is apparent that the preceding definition of the spatial correlation function refers to the average interaction between the wave fields at every pair of spatial points for which the distance is ξ and the center of symmetry locates at $\boldsymbol{r}$. By using Eq. (14) and taking the ensemble average over the whole bubble cloud, then, we define the total correlation function that is a function of the distance ξ so as to describe the overall correlation characteristics of the wave field. In respect that the normalized wave field $T(r)$ is symmetric about the origin, the total correlation function can be obtained by merely performing the integration with respect to r, given as below

$$C(\xi) = \frac{\int_0^R 4\pi r^2 g(\boldsymbol{r}+\boldsymbol{r}'/2,\boldsymbol{r}-\boldsymbol{r}'/2)dr}{\int_0^R 4\pi r^2 g(\boldsymbol{r},\boldsymbol{r})dr}. \tag{15}$$

III. THE NUMERICAL RESULTS

A set of numerical experiments has been carried out for various bubble radii, numbers, and volume fractions. Figure 3 presents the typical results of the total transmission and the total backscattering versus frequency kr_0 for bubbly gelatin with the parameters $N=200$, $r_0=1$ mm, and $\beta=10^{-3}$, respectively. The total transmission is defined as $I=\langle|T|^2\rangle$, and the received point is located at the distance $r=2R$ from the source. The total backscattering is defined as $\langle|\Sigma_i^N p_s^i(0)|^2\rangle$, referring to the signal received at the transmitting source. In the numerical experiments, the results are obtained at a series of discrete frequency points. The total number of the discrete frequency points in the spectral domain is 500.

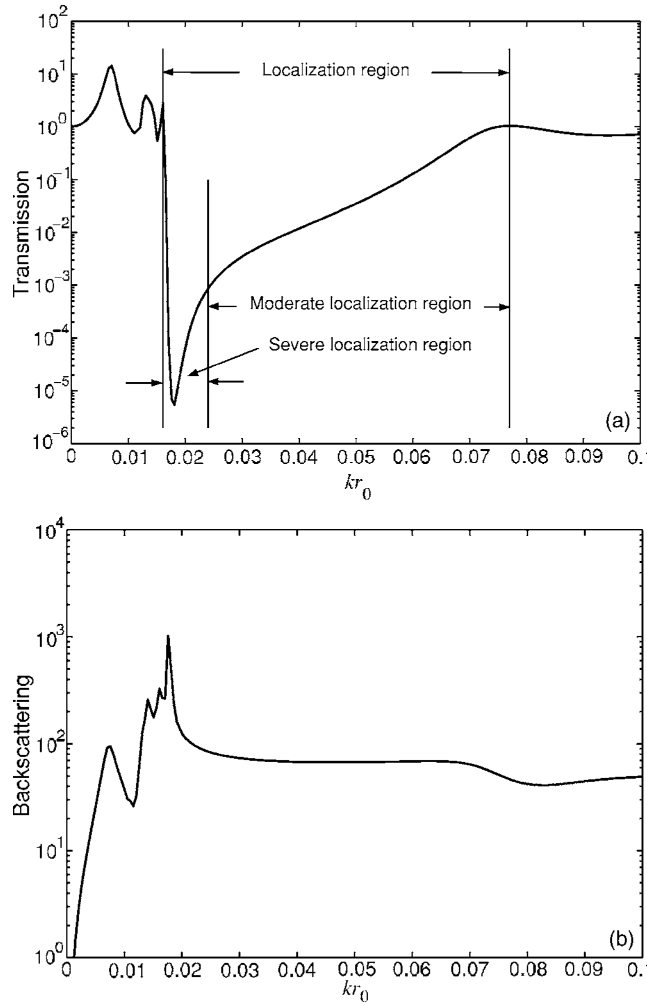

FIG. 3. The total transmission (a) and the total backscattering (b) versus frequency kr_0 for bubbly gelatin.

It is clearly suggested in Fig. 3(a) that there is a region of frequency slightly above the bubble resonance frequency, i.e., approximately between $kr_0=0.017$ and 0.077 in this particular case, in which the transmission is virtually forbidden. Within this frequency range, the Ioffe-Regel criterion is satisfied and a maximal decrease of the diffusion coefficient D roughly by a factor of 10^5 is observed and D can thus be considered having a tendency to vanish, i.e., $D\to 0$. Here the diffusion coefficient is defined [36] as $D=v_t l_{T_l}/3$ with v_t being the transport velocity that may be estimated by using an effective medium method [17]. Indeed, this is the range that suggests the acoustic localization where the waves are considered trapped [7], confirming the conjectured existence of the phenomenon of localization in such a class of media. Outside this region, wave propagation remains extended. For the backscattering situation, the result shows that the back-

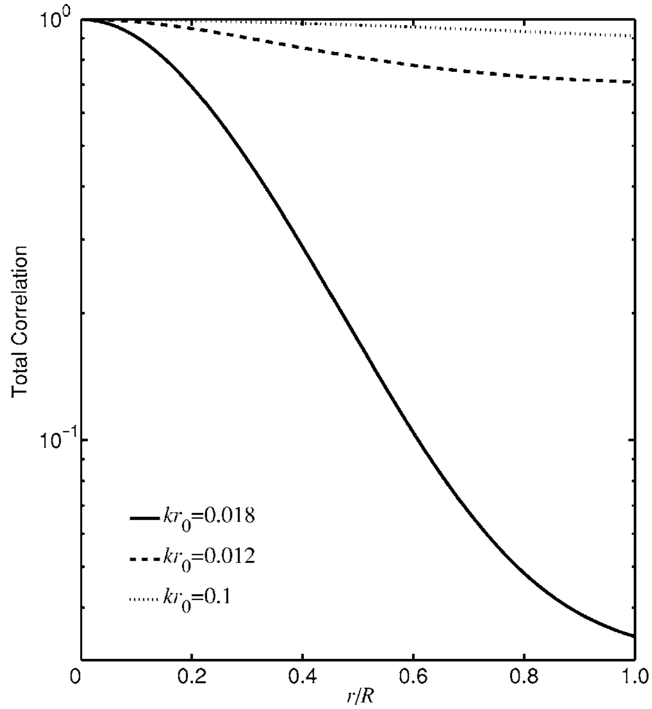

FIG. 4. The total correlation versus distance ξ for bubbly gelatin at three particular frequencies chosen as below, within, and above the localization region, respectively.

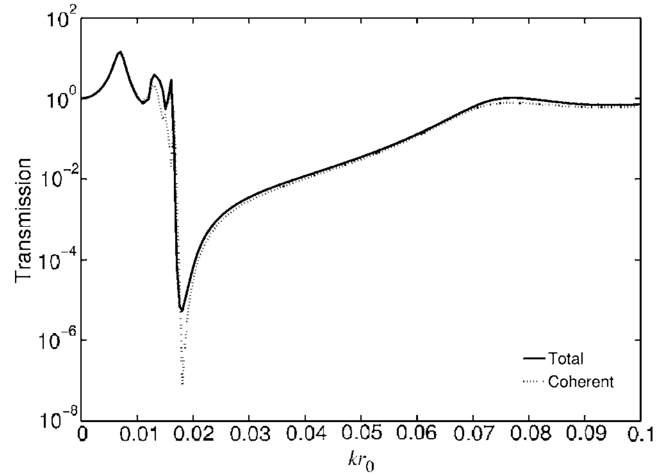

FIG. 5. The total transmission and the coherent portion versus frequency kr_0 for bubbly gelatin.

scattering signal persists for all the frequencies, and an enhancement of backscattering occurs particularly in the localization region. As has been suggested by Ye *et al.* [11], however, the backscattering enhancement that appears as long as there is multiple scattering cannot act as a direct indicator of the phenomenon of localization. In the following we shall thus focus our attention on the transmission that helps us to identify the localization regions, rather than the backscattering of the propagating wave.

Since the sample size is finite, the transmission is not completely diminished in the localization region, as expected [7]. In this particular case, there exists a narrow dip within the localization region between kr_0=0.017 and 0.024, hereafter termed severe localization region, in which the most severe localization occurs. The waves are moderately localized between kr_0=0.024 and 0.077, termed moderate localization region, due to the fact that the finite size of sample still enables waves in this region to leak out [10]. We find from Fig. 3 that for such systems of internal resonances, the waves are not localized exactly at the internal resonance, rather at parameters slightly different from the resonance. This indicates that mere resonance does not promise localization, supporting the assertion of Rusek *et al.* [5] and Alvarez *et al.* [12]. In fact, the acoustic localization in such systems is attributed to a collective behavior of bubbles [8,9].

To identify the phenomenon of localization by inspecting the correlation characteristics of the wave field in bubbly weakly compressible media, the total correlation functions are numerically studied for various frequencies and bubble parameters. Figure 4 illustrates the typical result of the comparison between the total correlation functions for bubbly gelatin at three particular frequencies chosen as below, within, and above the localization region: kr_0=0.012, 0.018, and 0.1, referring to Fig. 3. Here the parameters of bubbles are identical with those used in Fig. 3. Observation of Fig. 4 clearly reveals that the total correlation decays rapidly along the distance ξ in the case of kr_0=0.018, while the decrease of correlation with the increase of ξ is very slow in the cases of kr_0=0.012 and kr_0=0.1. Such spatial correlation behaviors may be understood by considering the coherent and the diffusive portions of the transmission. Here the coherent portion is defined as $I_C=|\langle T\rangle|^2$, and the diffusive portion is $I_D=I-I_C$. Figure 5 plots the total transmission and the coherent portion versus frequency kr_0 for bubbly gelatin with the parameters used in Fig. 4. It is obvious that the coherent portion dominates the transmission for most frequencies, while the diffusive portion dominates within the localization region. This is in good agreement with the conclusion drawn by Ye *et al.* for bubbly liquids (cf. see Fig. 1 in Ref. [7] and also Fig. 1 in Ref. [8]). As a result, there exist strong correlations between pairs of field points even for a considerable large distance within the non-localized region where the wave propagation is predominantly coherent. Contrarily, within the localization region almost all the waves are trapped inside a spatial domain and the fluctuation of wave field at a spatial point fails in interacting effectively with any other point far from it. These results suggest that proper analysis of the spatial correlation behaviors may serve for a way that helps discern the phenomenon of localization in a unique manner.

On the basis of appropriate analysis of the spatial correlation behaviors of the wave field, we have presented a method that suffices for the purpose of effectively identifying the localization phenomenon in bubbly weakly compressible media. In the following, however, the study of the localization phenomenon will be performed by examining the total transmission of the transmitting wave in order to obtain an overall physical picture. From the scattering function f of an individual bubble given by Eq. (6), we note that f is almost

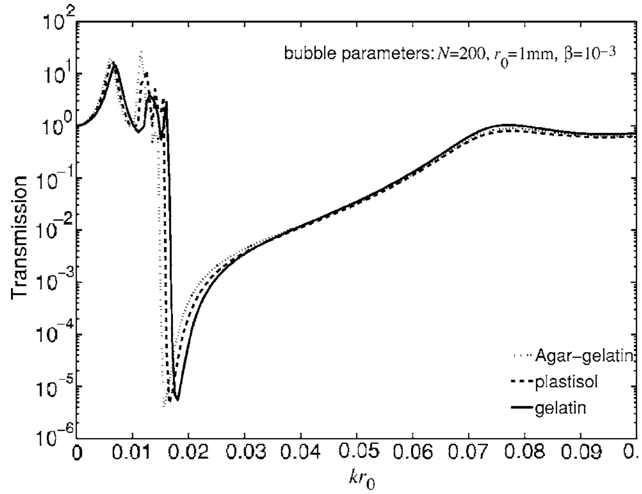

FIG. 6. The total transmission versus frequency kr_0 for three different kinds of bubbly weakly compressible media.

identical as the medium of matrix varies while keeping the bubble parameters constant, except that the bubble resonance frequencies ω_0 differ from each other owing to different values of shear moduli. Therefore it can be expected that acoustic localization should be a ubiquitous phenomenon in bubbly weakly compressible elastic media. Figure 6 shows the total transmissions versus frequency kr_0 for three different kinds of bubbly weakly compressible media: Agar-gelatin, plastisol, and gelatin. Here the parameters of bubbles are the same as in Fig. 3. Observation of Fig. 6 illustrates that the acoustic localization can be achieved in other kinds of bubbly weakly compressible media as well as in bubbly gelatin. Note from Fig. 2 that the resonance frequencies of an individual bubble in Agar-gelatin and plastisol are approximately $kr_0=0.0145$ and 0.015, respectively. As shown in Fig. 5, the acoustic localization regions of bubbly Agar-gelatin and bubbly plastisol are roughly $0.0155 \leq kr_0 \leq 0.076$ and $0.0165 \leq kr_0 \leq 0.0765$ respectively, slightly above the corresponding bubble resonance frequencies. It is obvious that the aforementioned features of localizations are qualitatively the same for different media except for different locations of localization regions.

To investigate how the wave propagation is affected as the bubble volume fraction varies, we plot in Fig. 7(a) the transmissions versus frequency kr_0 of a particular bubbly weakly compressible medium for three different volume fractions: $\beta=10^{-6}$, 10^{-4}, and 10^{-3}. The bubble radius $r_0=1$ mm. In Fig. 7, the weakly compressible medium is chosen as gelatin. It is obvious that the localization region has a tendency to shrink as the bubbles become more dilute. Compared with the case of volume fraction $\beta=10^{-3}$, the localization region is decreased from $0.017 \leq kr_0 \leq 0.077$ to $0.016 \leq kr_0 \leq 0.032$ when the volume fraction is decreased to $\beta=10^{-4}$. As the value of β becomes extremely small, the multiple scattering effect is severely weaken, hence the localization region tends to vanishes. For the case of volume fraction $\beta=10^{-6}$, significant inhibition is barely observable when compared to the case of $\beta=10^{-3}$, and the phenomenon of acoustic localization is absent. However, the phenomenon of localization appears as long as the bubble volume fraction is larger than 10^{-4}.

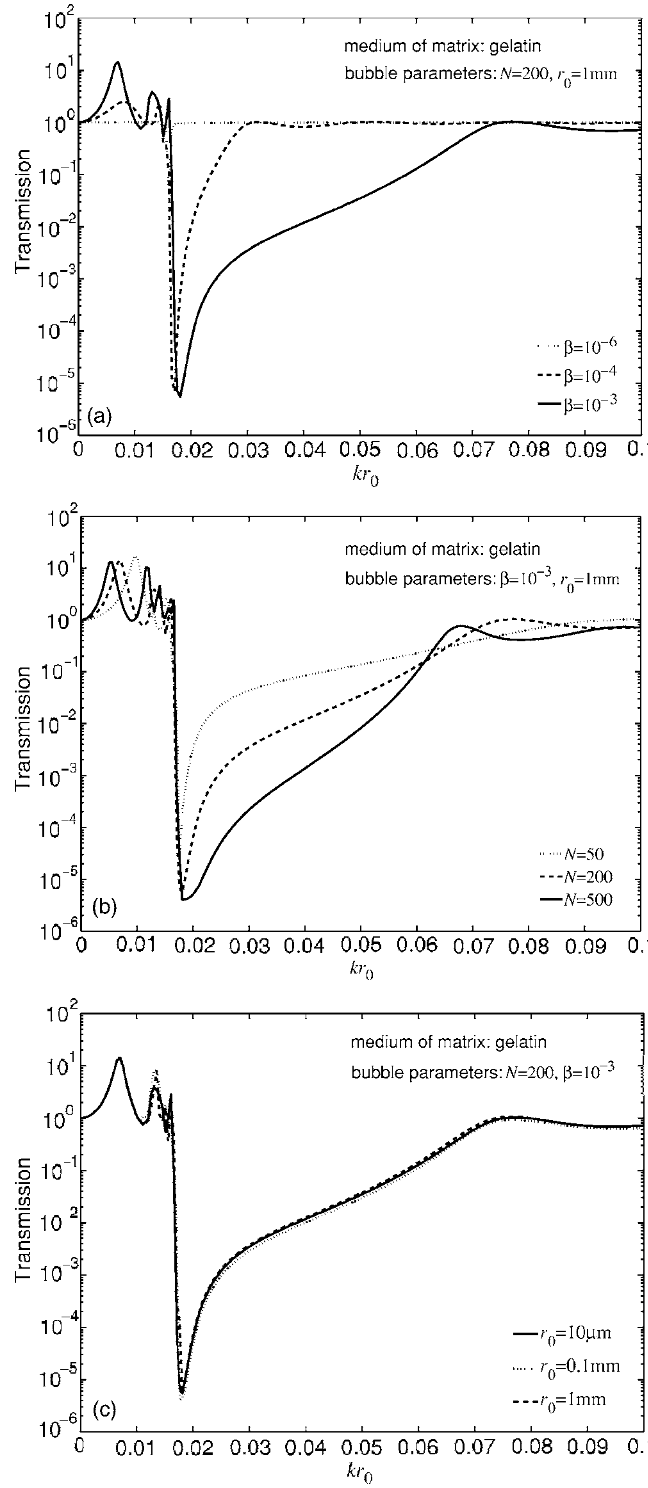

FIG. 7. The total transmission versus frequency kr_0 of bubbly gelatin for different bubble volume fractions (a), bubble numbers (b), and bubble sizes (c), respectively.

Note also that the lower limit of the localization regions is decreased from $kr_0=0.017$ to $kr_0=0.016$ and the locations of the greatest inhibition is also reduced from $kr_0=0.018$ to $kr_0=0.017$ as the volume fraction varies from $\beta=10^{-3}$ to 10^{-4}. Such a small shift in the position of localization region is due to the fact that the decrease (increase) of β is

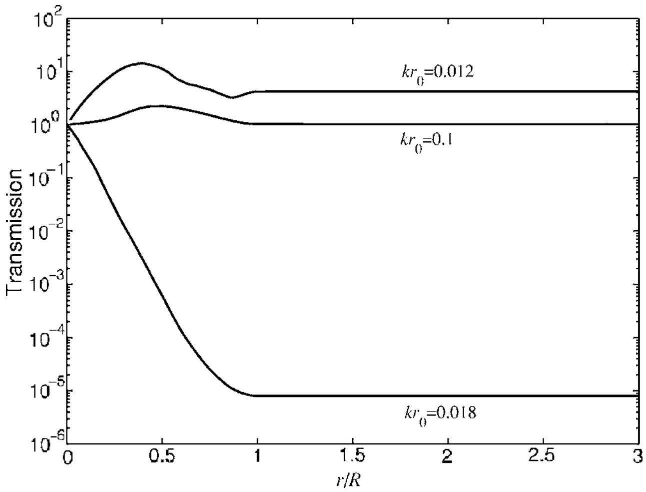

FIG. 8. The transmission as a function of distance from the source for bubbly gelatin at the three particular frequencies used in Fig. 3.

equivalent to the enlargement (reduction) of the average distance between bubbles.

In fact, any sample of bubbly weakly compressible medium is inevitably finite. Figure 7(b) displays the comparison of transmissions versus frequency kr_0 between three cases of different sample sizes, i.e., different bubble numbers: $N=50$, 200, and 500. The bubble radius $r_0=1$ mm and the volume fraction $\beta=10^{-3}$. The results show that acoustic localization takes effect for a small sample containing only 50 bubbles. The acoustic waves are localized within the frequency range between $kr_0=0.017$ and 0.09, and the corresponding severe localization region is between $kr_0=0.017$ and 0.019, as the dotted line shows in Fig. 7(b). When the sample size is increased, more waves within the localization region will be trapped, and the narrow dip corresponding to the severe localization region will be widened in result [10]. As illustrated by the comparison between the three lines in Fig. 7(b), the severe localization region is broadened to $0.017 \leq kr_0 \leq 0.034$ when the bubble number is increased to $N=500$. A sample containing 200 bubbles is considered sufficiently large for studying the phenomenon of localization. In the following computations, the bubble numbers are thus chosen as $N=200$.

The wave propagation in a particular medium is numerically computed for various bubble sizes, in which the radius of bubbles ranges from 10 μm to 1 mm. We find that all results are similar in this wide range of bubble radii. Figure 7(c) illustrates the typical result of the transmission versus frequency kr_0 for three particular bubble radii: $r_0=10$ μm, 0.1 mm, and 1 mm. The bubble volume fraction $\beta=10^{-3}$. It is evident in Fig. 7(c) that the curves of transmission are almost identical for the three bubble radii, indicating that the degree of localization in bubbly weakly compressible elastic media is insensitive to the bubble sizes.

We also examine the spatial distribution of acoustic energy and plot in Fig. 8 the transmission as a function of distance from the source at the three particular frequencies used in Fig. 3. In Fig. 8 we choose the bubble volume fraction $\beta=10^{-3}$ and bubble radius $r_0=1$ mm. Figure 8 shows that inside the bubble cloud, the total energy decays nearly exponentially along the distance of propagation when localization occurs, while the nonlocalized waves can propagate through the bubble cloud. Outside the bubble cloud, the transmissions remain constant in this region as they should. As a result, the waves are trapped within a spatial domain adjacent to the source once localized.

Finally a discussion will be made with regard to the influence of the absorption effects. In Eq. (1) the term $-(r_0/c_l)\cdot d^3U/dt^3$ in fact accounts for the radiation loss that stems from the weak compressibility of the medium [14,16]. The incorporation of various kinds of acoustic absorption such as thermal and viscosity effects amounts to adding a term $\nu dU/dt$ into the left-hand side of Eq. (1) [17]. Here ν is a coefficient characterizing the acoustic absorption. In such cases, the scattering function f given by Eq. (6) can be rewritten as follows:

$$f = \frac{r_0}{(\omega_0^2/\omega^2 - 1 - ikr_0 - i\delta)}, \tag{16}$$

where δ is the damping term that may be manually adjusted to inspect the sensibility of the results to the absorption effects.

Note that the scattering function given by Eq. (16) agrees in form with the scattering function of an air bubble in liquid with the damping term included [12]. A set of numerical experiments has been performed to investigate the influence of the absorption effects. The results show that: (1) The phenomenon of localization is not due to the absorption effects. This assertion is supported by the results of the present study, in which the damping term δ is set to be zero and the absorption effects are not taken into consideration. (2) Contrarily, the absorption effects will break the localization. As we manually increase the coefficient δ gradually, the phenomenon of localization becomes more difficult to be observed and eventually vanishes, which is consistent with the features of localization in a bubbly liquid [8].

IV. SUMMARY

The propagation of longitudinal acoustic waves in weakly compressible elastic media containing air bubbles is studied rigorously by incorporating all multiple scattering effects. The energy converted into shear wave is numerically proved negligible as the longitudinal wave is scattered by the bubbles. Under proper conditions, the acoustic localization can be achieved in such a class of media in a range of frequency slightly above the resonance frequency. Based on the analysis of the spatial correlation characteristic of the wave field, we present a method that helps to discern the phenomenon of localization in a unique manner. The features of localization are qualitatively the same for different media. The degree of wave trapping effect is sensitive to the frequency, the sample sizes and the bubble volume fraction, but relatively insensitive to the bubble sizes. The study of the spatial distribution of acoustic energy demonstrates that the localized waves are confined within a spatial domain near the source. As a result, an exponential decay of the transmission is observed as localization occurs.

ACKNOWLEDGMENTS

The work is supported by the Ministry of Education of China under Grant No. 705017, No. 20060284035, the Excellent Youth Science Foundation of China under Grant No. 10125417, and the State Key Development Program of Basic Research of China under Grant No. 51315.

[1] P. W. Anderson, Phys. Rev. **109**, 1492 (1958).
[2] R. Dalichaouch, J. P. Armstrong, S. Schultz, P. M. Platzman, and S. L. McCall, Nature (London) **354**, 53 (1991).
[3] A. Z. Genack and N. Garcia, Phys. Rev. Lett. **66**, 2064 (1991).
[4] D. S. Wiersma, P. Bartolini, A. Lagendijk, and R. Roghini, Nature (London) **390**, 671 (1997).
[5] M. Rusek, A. Orlowski, and J. Mostowski, Phys. Rev. E **53**, 4122 (1996).
[6] D. Sornette and B. Souillard, Europhys. Lett. **7**, 269 (1988).
[7] Z. Ye and A. Alvarez, Phys. Rev. Lett. **80**, 3503 (1998).
[8] Z. Ye and H. Hsu, Appl. Phys. Lett. **79**, 1724 (2001).
[9] C. H. Kuo, K. K. Wang, and Z. Ye, Appl. Phys. Lett. **83**, 4247 (2003).
[10] K. X. Wang and Z. Ye, Phys. Rev. E **64**, 056607 (2001).
[11] Z. Ye, H. Hsu, and E. Hoskinson, Phys. Lett. A **275**, 452 (2000).
[12] A. Alvarez and Z. Ye, Phys. Lett. A **252**, 53 (1999).
[13] L. D. Landau and E. M. Lifshits, *Theory of Elasticity* (Pergamon, Oxford, 1986).
[14] L. A. Ostrovsky, Sov. Phys. Acoust. **34**, 523 (1988).
[15] L. A. Ostrovsky, J. Acoust. Soc. Am. **90**, 3332 (1991).
[16] E. A. Zabolotskaya, Y. A. Ilinskii, G. D. Meegan, and M. F. Hamilton, J. Acoust. Soc. Am. **118**, 2173 (2005).
[17] B. Liang, Z. M. Zhu, and J. C. Cheng, Chin. Phys. **15**, 412 (2006).
[18] C. F. Ying and R. Truell, J. Appl. Phys. **27**, 1086 (1956).
[19] G. C. Gaunaurd, K. P. Scharnhorst, and H. Überall, J. Acoust. Soc. Am. **65**, 573 (1979).
[20] D. M. Egle, J. Acoust. Soc. Am. **70**, 476 (1981).
[21] R. L. Weaver, J. Acoust. Soc. Am. **71**, 1608 (1982).
[22] K. Busch, C. M. Soukoulis, and E. N. Economou, Phys. Rev. B **50**, 93 (1994).
[23] C. A. Condat, J. Acoust. Soc. Am. **83**, 441 (1988).
[24] G. C. Gaunaurd and H. Überall, J. Acoust. Soc. Am. **63**, 573 (1978).
[25] D. Brill, G. C. Gaunaurd, and H. Überall, J. Acoust. Soc. Am. **67**, 414 (1980).
[26] N. G. Einspruch and R. Truell, J. Acoust. Soc. Am. **32**, 214 (1960).
[27] A. A. Asatryan, P. A. Robinson, R. C. McPhedran, L. C. Botten, C. Martijin de Sterke, T. L. Langtry, and N. A. Nicorovici, Phys. Rev. E **67**, 036605 (2003).
[28] S. Gerristsen and G. E. W. Bauer, Phys. Rev. E **73**, 016618 (2006).
[29] S. Catheline, J. L. Gennisson, and M. Fink, J. Acoust. Soc. Am. **114**, 3087 (2003).
[30] Z. Fan, J. Ma, B. Liang, Z. M. Zhu, and J. C. Cheng, Acust. Acta Acust. **92**, 217 (2006).
[31] I. Y. Belyaeva and E. M. Timanin, Sov. Phys. Acoust. **37**, 533 (1991).
[32] G. C. Gaunaurd and H. Überall, J. Acoust. Soc. Am. **71**, 282 (1982).
[33] A. Alvarez, C. C. Wang, and Z. Ye, J. Comput. Phys. **154**, 231 (1999).
[34] L. L. Foldy, Phys. Rev. **67**, 107 (1945).
[35] A. Ishimaru, *Wave Propagation and Scattering in Random Media* (Academic Press, New York, 1978).
[36] B. C. Gupta and Z. Ye, Phys. Rev. E **67**, 036606 (2003).